Quantum Interference of Electrons in Fibrous Ta_4Te_4Si

Quasi-one-dimensional compounds attract considerable attention due to various electronic instabilities such as charge and spin density waves and unusual 'normal' phase features. For example, two charge density waves with incommensurate lattice distortions along the chain direction have been observed in inorganic compound $NbSe_3$. In the organic conductors $(TMTSF)_2X$, known as Bechgaard salts, states with spin density wave, metallic conductivity and superconductivity were found at different pressure and magnetic field. However, some quasi-one-dimensional compounds remain stable against such symmetry-breaking instabilities. For example, the compounds $Hg_{3-\delta}AsF_6$, $TaSe_3$, $Tl_2Mo_6Se_6$ remain metallic down to 4 K and even exhibit superconductivity at lower temperatures. A search for other one-dimensional systems which are resistant to electronic and structural instabilities therefore is of particular interest.

In this context we focussed our attention on the quasi one-dimensional compound Ta_4Te_4Si. The crystal structure of Ta_4Te_4Si contains Si centered square antiprismatic Ta_4Te_4 infinite chains which are weakly coupled to neighboring chains via Te-Te van der Waals interaction (Fig. 1). According to band-structure calculations the structure should be stable and metallic with two half-filled and a twofold degenerate nearly filled conduction band. However, early resistivity measurements showed resistivity characteristics similar to those in $NbSe_3$ and pointed to an electronic and structural instability in Ta_4Te_4Si as well.

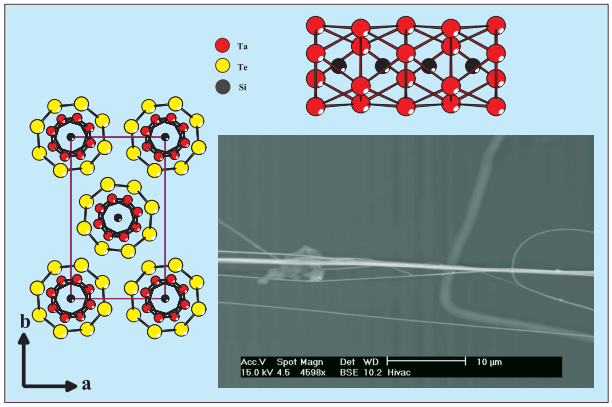

Figure 1: Left: Projection of the crystal structure of Ta_4Te_4Si along [001]. Right top: Part of an infinie Ta-Si strand extending along [001]. Right bottom: Electron microscope graph of Ta_4Te_4Si fibers.

Here we present a magnetoresistance study of crystalline Ta_4Te_4Si fibers (typical thickness $< 5\,\mu m$). Both, the temperature dependence of the resistivity and the magnetoresistance prove metallic behavior down to 1.7 K. The low-field magnetoresistance is interpreted in terms of three-dimensional anisotropic weak-localization theory. Carrier phase scattering lengths extracted from the magnetoresistance data are in good agreement with theoretical predictions for electron-electron interactions in disordered metals.

Figure 2 shows a typical temperature dependence of the resistance in the range 1.7–300 K. Starting from room temperature the resistance gradually decreases with T and saturates below 10 K typical for metallic behavior (curve 1 in Fig. 2). The low-temperature resistivity value $0.92 \times 10^{-4}\,\Omega\,cm$ is characteristic for semimetals.

Close inspection of the low-temperature region reveals a weak temperature dependence of resistivity which is essentially sample dependent. For samples A and B resistivity increases and decreases, respectively, by 0.5% and 0.02% in the range 1.7–4 K as shown in the inset of Fig. 2. The magnitude of this effect and its low temperature character allow us to connect it with the quantum interference corrections to the resistivity. These effects are very sensitive to lattice defects which can lead to qualitatively different behavior of different fibers from the same batch. Resistivity anomalies at ≈ 200 K are only observed after the fibers have been exposed to a current pulse of

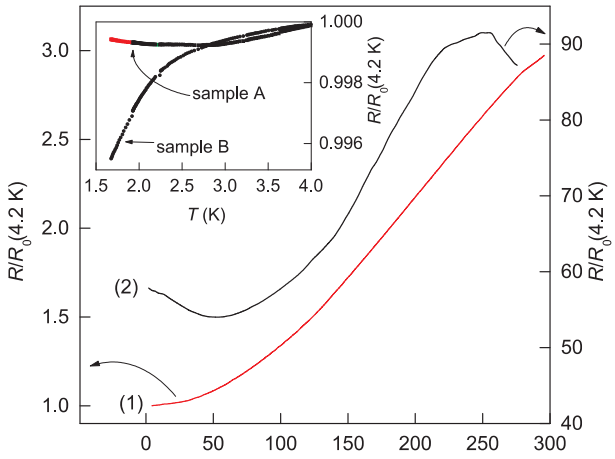

Figure 2: Temperature dependence of the magnetoresistance before (1) and after (2) application of a current pulse of $\approx 10^5$ A/cm^2. Low temperature resistances of two different sampes are shown in the inset.

$>10^5$ A/cm^2. For the following magnetoresistance investigation, we have selected such fibers with a clear metallic temperature characteristic.

Figure 3(a) shows the resistance as a function of the magnetic field H. The overall magnetoresistance $(R(H_i) - R(0))/R(0)$ is positive with the classical mechanism dominating above 5 T. The sharp dip in fields $H < 1$ T is a fingerprint of the suppression of weak localization by magnetic field. Given that the large-scale electron coherence length L_φ is usually 10–1000 nm, magnetic fields of the order of $\hbar/4eL_\varphi^2$ are necessary for a suppression. The broadening of the magnetoresistance dip with increasing temperature reflects the decrease of L_φ due to both electron-electron and electron-phonon scattering. The magnetoresistance is anisotropic due to the chain structure of the compound: In fields parallel to the chains the dip is always broader (i.e. L_φ is shorter) than in the perpendicular field orientation. The anisotropy in the plane perpendicular to the chain is 10% or less.

To model the magnetoresistance data we used anisotropic three-dimensional theory of quantum interference corrections to resistivity. It includes weak localization and electron-electron interaction effects. In the limit of low fields and strong spin-orbit scattering the relative change of the resistance for the current along the chain axis is expressed by

$$\frac{R(H_i) - R(0)}{R(0)} = \alpha_i \rho_0 \frac{e^2}{4\pi^2\hbar}\gamma^{3/4}\frac{1}{L_{\varphi\,-}} f_3\left(\frac{4eL_{\varphi\,i}^2 H_i}{\hbar}\right)\sqrt{\frac{4eL_{\varphi\,i}^2 H_i}{\hbar}} + BH_i^2, \qquad (1)$$

where the index $i = -$ or $\|$ in H_i, α_i and $L_{\varphi\,i}$ indicates the direction of the magnetic field with respect to the chain axis, $L_{\varphi\,i}$ are connected with the phase-braking time τ_φ via the relations $L_{\varphi\,\|} = \sqrt{D_t\tau_\varphi}$ and $L_{\varphi\,-} = (D_t D_l)^{1/4}\sqrt{\tau_\varphi}$ with the diffusion constants D_t and D_l perpendicular and parallel to the chain axis, $\gamma = D_l/D_t$, and $f_3(1/x) = 2[\sqrt{2+x} - \sqrt{x}] - [(0.5+x)^{-1/2} + (1.5+x)^{-1/2}] + (2.03+x)^{-3/2}/48$. The first term in Eq. (1) describes the weak antilocalization correction in the singlet channel of electron diffusion. This term with $\alpha = 0.5$ is dominant for heavy element compounds where spin-orbit scattering time τ_{so} is much shorter than τ_φ. The second, quadratic term contains contributions from the classical magnetoresistance mechanism, weak localization in the triplet channel, spin splitting and electron-electron scattering in the limit of low fields, $H \ll \hbar/4eD\tau_{so}$, $H \ll k_B T/g\mu_B$ and $H \ll \pi k_B T/2eD$ where k_B is the Boltzmann constant, μ_B is the Bohr magneton, and g is the gyromagnetic ratio.

We fit the magnetoresistance data to Eq. (1) using α_i, $L_{\varphi\,i}$, and B as fitting parameters. These fits (see Fig. 3(b)) are in very good agreement with the experimental data for all temperatures and for both orientations of the magnetic fields. The standard deviation value of 6×10^{-6} is comparable

with the measurement accuracy. Other models of the magnetoresistance describe experimental dependences much worse. For example, the one-dimensional weak localization correction with the quadratic classical magnetoresistance term $[R(H)-R(0)]/R(0) = a_1(1+(H/a_2)^2)^{-1/2}-a_1+a_3H^2$ ($a_1 = -7.03\times10^{-4}$, a_2 =85.4 mT, $a_3 = 3.21\times10^{-4}$ T^{-2}) gives 3.4 times larger standard deviation and does not fit the experimental behavior both in low and high field regions (see the dashed curves in Fig. 3(b) and in its inset).

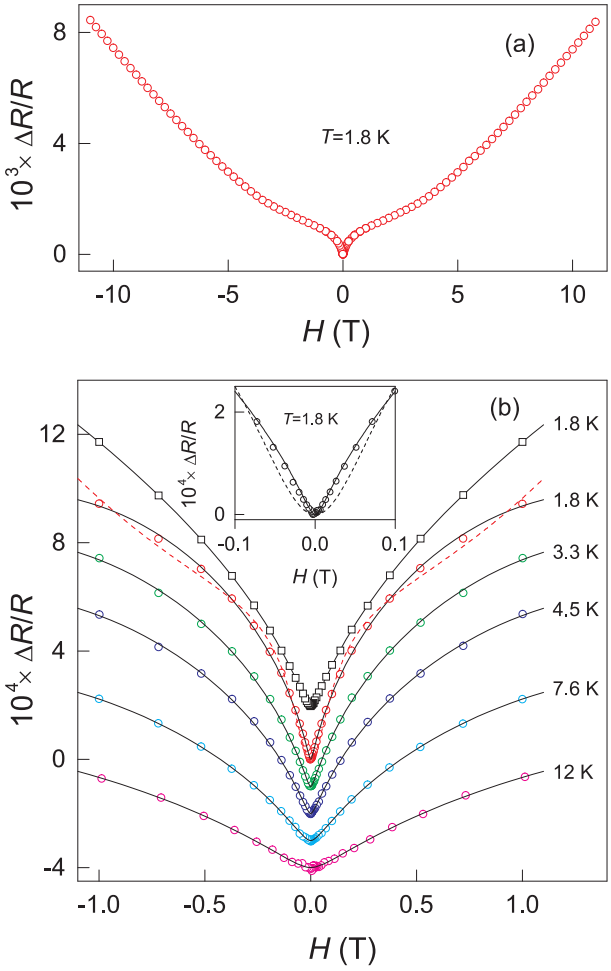

Figure 3: The normalized magnetoresistance $\Delta R/R = [R(H) - R(0)/R(0)]$ of sample A, aligned along (□) and perpendicular (○) to the crystallographic c-axis. (a) Magnetoresistance in the range of fields up to 11 T. (b) Magnetoresistance in the range of fields up to 1 T for various temperatures. The symbols present experimental data and the solid lines are fits to Eq. (1) for three-dimensional weak localization corrections (Curves and symbols are shifted vertically for better visibility) The dashed line is the best fit of the 1.8 K data to one-dimensional weak localization corrections. Inset: Magnetoresistance in the range of fields up to 0.1 T with one-dimensional and three-dimensional weak localization corrections for comparison.

The anisotropy of magnetoresistance was measured only at the lowest temperature $T = 1.8$ K to diminish the overlap of the quantum mechanical and classical magnetoresistance components in the case of the parallel field orientation. In sample A we receive $L_{\varphi\parallel} = 137$ nm, $L_{\varphi\perp} = 246$ nm, and $\gamma = 10$. The anisotropy of samples B and C is larger – $\gamma = 17$ and 29, respectively. In the subsequent analysis these values will be used for temperatures up to 15 K. In this range the resistivity saturates which points to the constant value of the diffusion constant. α_i depends on the direction of magnetic field and the ratio $\alpha_\parallel/\alpha_\perp$ is 1.8, 2.2 and 1.9 in samples A, B and C,

respectively. Possibly, this anisotropy indicates the nonuniversal behavior of the three-dimensional weak-localization.

Above 10 K the coefficient α_- in Eq. (1) reaches values 0.24–0.44, close to the theoretical value $\alpha_- = 0.5$, if we take into account the uncertainty of ρ_0. With decreasing temperature, α_- increases for all samples. This effect is particularly noticeable for sample B for which α_- growth steeply below 2.5 K. This strong temperature dependence which correlates with the temperature dependence of the resistance (see inset of Fig. 2) suggests that this behavior is connected with scattering on virtual Cooper pairs at $T > T_c$ (Maki-Thompson-Larkin effect). Strong superconducting fluctuations allow us to expect the superconducting transition in this compound at sub-Kelvin temperatures. Further experiments are deviced to verify this presumption.

In summary, we investigated the electrical properties of Ta_4Te_4Si fibers and found that Ta_4Te_4Si is intrinsically metallic down to 1.7 K. From a detailed analysis of the magnetoresistance we conclude that in the temperature range 3–15 K electron decoherence is best described by the theory of electron-electron scattering. The quantum interference contribution to the magnetoresistance can be interpreted in the framework of three-dimensional weak localization theory in the limit of strong spin-orbit scattering. Resistivity anomalies previously ascribed to charge density wave like anomalies are most likely due to crystalline imperfections induced by current pulses.

(A. Stolovits (Tartu Estonia), A. Sherman (Tartu, Estonia), K. Ahn and R. K. Kremer)